Isomerization of Cyclopropanecarbonitrile. Quantum Chemical and Model Calculations

Faina Dubnikova and Assa Lifshitz*

Department of Physical Chemistry, The Hebrew University, Jerusalem 91904, Israel

Received: February 16, 1998; In Final Form: April 24, 1998

Density functional theory (DFT) and two-configuration self-consistent-field (TCSCF) calculations including CI were carried out to investigate the pathways of the unimolecular isomerizations of cyclopropanecarbonitrile. Vibrational frequencies calculated at DFT and TCSCF levels of theory were used to estimate frequency factors by transition state theory. Transition states corresponding to both closed shell, concerted and biradical paths in the formation of the main products (*cis*- and *trans*-crotonitrile and vinylacetonitrile) were localized. However, owing to Hartree−Fock instabilities in the wave functions of the closed shell (concerted) transition states, it is not clear whether the concerted path is of any physical significance. RRKM calculations were carried out to transfer values of A_∞ and E_∞ of the isomerizations to A and E_a corresponding to the experimental conditions. Computer modeling, containing the biradical isomerization pathway and the interisomerizations between the products, was carried out, and the results are compared with the experiment. Methacrylonitrile, which is formed in trace quantities, proceeds via a concerted mechanism with a closed shell singlet transition state but with some contribution of a biradical character.

I. Introduction

The unimolecular isomerization of three-membered rings have long been a subject of detailed quantum chemical calculations. The main effort in these calculations was devoted to the geometrical and optical isomerizations of cyclopropane and substituted cyclopropanes.[1−8] It has been shown that these isomerizations proceed via a biradical mechanism with the formation of a short-lived 1,3-biradical intermediate. On the other hand, very little has been done in trying to evaluate transition states of structural isomerizations although there is a considerable volume of experimental results on these isomerizations.[9−15] Only recently such transition states were reported on the structural isomerization cyclopropane → propylene.[16,17] We are not aware of any quantum chemical calculations of transition states of the structural isomerizations of substituted cyclopropanes. For the latter the structural isomerizations may lead to the production of several isomers, depending upon the position of the broken bond and the nature of the H-atom migration with respect to the functional group on the ring.

This investigation deals with the structural isomerization of cyclopropanecarbonitrile (CPCN). The latter was studied experimentally both at low and at high temperatures using a static system at low temperatures (660−760 K)[13] and the single-pulse shock tube at high temperatures (900−1050 K).[14] The isomerization of cyclopropanecarbonitrile yields *cis*- and *trans*-crotonitrile ($CH_3CH{=}CNCN$) (CRNT), vinylacetonitrile ($CH_2{=}CHCH_2CN$) (VACN), and trace quantities of methacrylonitrile ($CH_2{=}C(CH_3)CN$) (MACN). In addition, there is an interisomerization among the products. The main isomerizations were found to proceed with an activation energy of some 8 kcal/mol lower than that of cyclopropane.[14] This fact was attributed to the resonance stabilization of the biradical transition states and the intermediate by the CN group.[13,14]

In the present investigation we report on quantum chemical calculations of the reaction paths in the unimolecular structural rearrangements of cyclopropanecarbonitrile and on the interisomerization among the products. We also report on modeling calculations using the computed rate parameters and compare the results with the experimentally measured isomerization rates.

II. Computational Details

Optimization of the ground-state geometry of cyclopropanecarbonitrile and its isomerization products, as well as the geometry of the intermediate and the transition states of the reactions under consideration, was carried out using a density functional theory (DFT) employing the B3LYP (Becke three-parameter hybrid method,[18] with Lee−Yang−Parr correlation functional approximation[19]) by means of the Berny geometry optimization algorithm. The DFT computations were carried out using the Gaussian-94 program package.[20]

We have tested several methods and several basis sets before choosing the method and basis set for the present calculations. In addition to DFT, MP2 calculations with frozen core approximation were also carried out. Two basis sets were tested with these methods: the standard Pople polarized split-valence 6-31G**[21] and the Dunning correlation consistent polarized valence double ζ (cc-pVDZ) basis sets.[22,23] All the calculations were performed without symmetry restrictions. Vibrational analyses were carried out at the same level of theory to characterize the optimized structures as local minima or transition states. Each optimized structure was recalculated at single-point quadratic CI calculations including single and double substitutions with a triplet contribution to the energy—QCISD(T).[24] QCISD(T) calculations were performed with frozen core approximation.

As has been done in cyclopropane isomerization,[25] we used an open-shell singlet approximation for calculating the intermediate and the transition states. Biradical structures were localized by using guess wave function with the destruction $\alpha-\beta$ and spatial symmetries by unrestricted uB3LYP method and were recalculated also by the single-point uQCISD(T) method.

Because the DFT methods are less sensitive to multireference effects, we performed also full optimization to all the biradical structures using two-configuration self-consistent-field (TCSCF)

S1089-5639(98)01152-9 CCC: $15.00
Published on Web 06/20/1998

method with the cc-pVDZ basis set. The reference configuration was defined by filling separately the α and β occupied orbitals (six singlet configurations). The initial guess wave functions were taken from unrestricted Hartree−Fock (uHF) calculations at optimal uB3LYP geometry. The TCSCF calculations were carried out using the Gamess-USA program.[26]

Calculated vibrational frequencies and entropies (at uB3LYP and TCSCF levels) were used to evaluate preexponential factors of the reactions under consideration. All the calculated frequencies as well as the zero-point energies are of harmonic oscillators. The calculated frequencies were not scaled. The calculations of the intrinsic reaction coordinate (IRC) were done at the uB3LYP level of theory with mass-weighted internal coordinates, to make sure that the transition states connect the desired reactants and products. Only this coordinate system permits to follow to steepest descent path.[27] We computed the IRC path using the same basis set that was used for the stationary point optimization.

All the calculations were carried out on a DEC Alpha TurboLaser 8200 5/300 at the Institute of Chemistry of The Hebrew University of Jerusalem.

III. Reactant and Products

Table 1 shows selected experimental[28] and calculated parameters of cyclopropanecarbonitrile using the B3LYP and MP2 levels of theory with two basis sets, 6-31G* and cc-pVDZ. As can be seen the structural parameters when calculated with MP2/6-31G** are in less agreement with the experimental structure than when calculated using B3LYP with both 6-31G** and cc-pVDZ basis sets. For the latter the overall agreement with the experimentally measured bond lengths and bond angles is very good. However, all the methods and basis sets that were used in the calculations overestimate the distance between the cyclopropane ring and the CN group (r-$_{C(3)-C(4)}$) by about 0.02 Å. The best agreement between the calculations and the experiment[29] also for the frequency calculations was obtained when using B3LYP/cc-pVDZ (Table 2). The B3LYP/cc-pVDZ frequencies are also in good agreement with measured values of the isomerization products. Table 3 shows the experimental[31] and calculated frequencies of *cis*- and *trans*-crotonitrile (only at the B3LYP/cc-pVDZ level of theory). Except for unclear deviation in one fundamental frequency the agreement is very good. (Experimental frequencies for vinylacetonitrile are unavailable).

TABLE 1: Comparison between the Structural Parameters of Cyclopropanecarbonitrile Obtained Experimentally[28] and Evaluated at Different Computational Levels

parameter[a]	B3LYP/ 6-31G**	B3LYP/ cc-pVDZ	MP2/ 6-31G**	exptl[b]
r-C(1)C(3)[c]	1.522	1.524	1.513	1.529
r-C(1)C(2)	1.498	1.501	1.494	1.501
r-C(3)C(4)	1.441	1.443	1.441	1.420
r-C(4)N	1.163	1.163	1.182	1.161
∠C(2)C(3)C(4)	119.5	119.4	119.0	118.7
∠C(3)C(4)N	179.8	179.7	179.1	179.3

[a] Distances in angstroms, angles in degrees. [b] Experimental parameters from ref 28. [c] The atoms are numbered as shown in Figure 2.

As can be seen (Tables 2 and 3), the scaling of the calculated frequencies did not improve the agreement with the experiment. On the contrary, the percent deviations of the unscaled (raw) frequencies are smaller. We have thus chosen the B3LYP method and the cc-pVDZ basis set for all our calculations without frequency scaling. The same basis set was also used with the TCSCF method. The calculated geometrical parameters at the B3LYP/cc-pVDZ level of theory of the reactant and all the products are summarized in Table 4. The calculated frequencies of vinylacetonitrile and methacrylonitrile are shown in Table 5. The calculated moments of inertia, entropies, and ZPE of the reactant and all the products are shown in Table 6; total and relative energies are shown in Table 7. These values served for calculating the Arrhenius parameters and activation energies for the kinetic modeling.

IV. Biradical Pathways of Cyclopropanecarbonitrile Isomerization

A. Structures of the Critical Points along the Pathways of the Main Product Formation. Schematic representation of the isomerization of cyclopropanecarbonitrile based on a biradical mechanism is shown in Figure 1. The formation of *cis*- and *trans*-crotonitrile and vinylacetonitrile takes place via biradical trimethylene intermediate whereas the production of methacrylonitrile proceeds via a biradical, open shell singlet transition state but without an intermediate. The existence of an intermediate in the first four channels was established by IRC analysis. The analysis of the optimized transition states TS1−TS5 led to the same trimethylene cyanide intermediate INT1 regardless of whether the starting point was TS1 (connecting to the reactant) or TS2−TS5 (connecting to the products). TS1 connected the reactant to the biradical intermediate and not to *cis*- or *trans*-crotonitrile or to vinylacetonitrile.

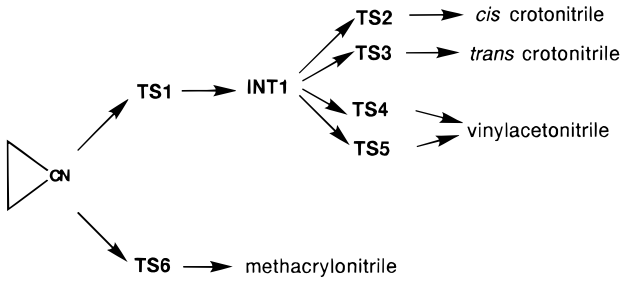

Figure 1. Schematic presentation of the cyclopropanecarbonitrile isomerizations.

The geometrical parameters of the calculated transition states TS1-TS5 and of the intermediate INT1 are shown in Tables 8 (uB3LYP-optimized) and 9 (TCSCF-optimized). Although the exact bond lengths and angles in the two methods of calculations are not exactly the same, both methods show the same variation in structure along the reaction paths.

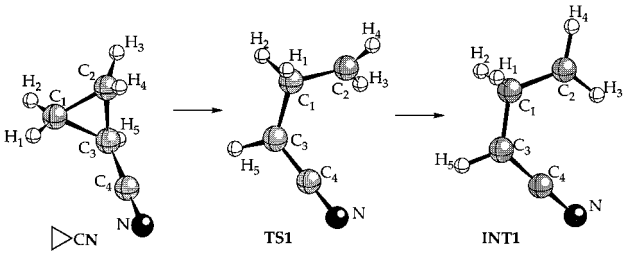

Figure 2. Structure of cyclopropanecarbonitrile, TS1, and the intermediate INT1. This route represents the first step of the C_3H_5CN manifold for the main isomerization products.

The first stage of the isomerization is comprised of the two CN-substituted trimethylenes (Figure 2), the ring-opening transition state TS1, and the intermediate INT1. The TS1 structure is edge-to-face (EF, or "0,90") and the intermediate is an edge-to-edge (EE, or "0,0") conformer. The reaction coordinate in

TABLE 2: Experimental[29] and Calculated Frequencies of Cyclopropanecarbonitrile (in cm^{-1}) by Different Methods and Basis Sets

	B3LYP/cc-pVDZ			B3LYP/6-31G**			MP2/6-31G**			
exptl[a]	raw	Δ^b %	$\Delta^{b,c}$ %	raw	Δ^b %	$\Delta^{b,c}$ %	raw	Δ^b %	$\Delta^{b,d}$ %	mode description[e]
(222)	213	−4.1	−7.7	215	−3.2	−6.8	207	−6.8	−12.2	C(CN) wag/N≡CC bend
222	215	−3.2	−6.8	217	−2.3	−5.9	213	−4.1	−9.5	N≡CC bend/CCN rock
(527)	527	0.0	−3.0	530	0.6	−3.4	524	−5.7	−6.3	CCN rock/N≡CC bend
(543)	548	0.9	−2.9	552	3.9	−2.2	538	−0.9	−6.4	N≡CC bend/C(CN) wag
736	753	2.3	−1.6	759	3.1	−0.8	780	6.0	0	C−CN stretch
808	808	0.0	−3.8	816	1.0	−3.1	838	3.7	−2.0	CH_2 rock
821	819	−0.2	−4.1	829	1.0	−2.9	861	4.9	−1.1	CH_2 rock
(880)	898	2.0	−1.9	906	3.0	−1.0	949	7.8	2.4	ring deformation
941	963	2.3	−1.6	976	2.8	−1.2	1002	6.5	0.4	ring deformation
1049	1057	0.8	−3.1	1093	4.2	0.2	1120	6.8	0.8	CH_2 wag
1070	1072	0.2	−3.7	1077	0.6	−3.3	1126	5.2	−0.7	CH_2 wag
1088	1097	0.9	−3.1	1116	2.6	−1.4	1159	5.1	0.5	CH bend
(1125)	1128	0.3	−3.6	1143	1.6	−2.3	1167	3.7	−2.1	CH_2 twist
(1180)	1187	0.6	−3.1	1206	2.2	−1.8	1242	5.3	−0.7	CH_2 twist
1195	1212	1.4	−2.5	1222	2.3	−1.7	1260	5.7	−0.2	ring breaching
(1344)	1368	1.8	−3.8	1390	3.3	−0.6	1425	8.0	0.0	CH bend
1442	1438	0.3	−4.2	1482	2.8	−1.1	1525	5.8	−0.2	CH_2 deformation
1468	1482	1.0	−3.9	1518	3.4	−0.6	1566	6.7	0.6	CH_2 deformation
2264	2352	3.9	−0.1	2360	4.2	0.2	2216	2.1	−7.7	CN stretch
3040	3141	3.3	−0.7	3156	3.8	0.0	3242	6.6	0.6	CH_2 symmetric stretch
3044	3137	3.1	−0.9	3159	3.8	−0.2	3247	9.0	0.6	CH_2 symmetric stretch
(3052)	3166	3.7	−0.3	3178	4.2	0.0	3273	7.2	1.2	CH stretch
(3094)	3228	4.3	0.3	3241	4.8	0.7	3341	8.0	1.9	CH_2 antisymmetric stretch
3120	3242	3.9	−0.1	3254	4.3	0.3	3352	7.4	1.3	CH_2 antisymmetric stretch

[a] Gas-phase frequencies (exptl). Values in parentheses obtained in the liquid phase.[29] [b] Δ = (calculated value − experimental value)/experimental value, in percent. [c] Scaling factor is 0.9434.[30] [d] Scaling factor is 0.9613.[30] [e] Mode description from ref 29.

TABLE 3: Experimental[31] and Calculated Frequencies of *cis*- and *trans*-Crotonitrile (in cm^{-1}) at B3LYP/cc-pVDZ

trans-crotonitrile				*cis*-crotonitrile				
exptl[a]	raw	Δraw[b] %	Δscale[c] %	exptl[a]	raw	Δraw[b] %	Δscale[c] %	mode description[d]
173	175	1.1	−2.8	154	158	2.6	−1.4	C−C≡N bend
181[e]	178	1.7	−5.5	219[e]	160	−36.9	−29.8	CH_3 torsion
246[e]	205	−16.7	−19.9	278	292	5.0	1.0	C−C≡N bend
398	397	−0.2	−4.1	398[f]	395	−0.7	−4.6	C=C−CH_3 bend
461	498	8.0	3.8	517	533	3.0	−0.9	C=C−CH_3 bend
555	559	0.1	−3.2	658	665	1.1	−2.8	C=C−CN bend
788	805	2.2	−1.8	726	750	3.3	−5.0	HCCH symmetrical bend
896	908	1.3	−2.6	892	909	−1.9	−2.0	C−CN stretch
957	985	2.9	−1.1	954	968	1.5	−2.5	HCCH unsymmetrical bend
1023	1044	2.1	−1.9	1232	1250	1.4	−2.5	C−CH_3 stretch
1044	1058	1.3	−2.6	1034	1056	2.1	−1.8	CH_3 rock
1115	1130	1.3	−2.6	1104[f]	1115	1.0	−2.9	CH_3 rocking
1288	1291	0.2	−3.6	1399	1412	0.9	−3.0	HCCH unsymmetrical deformation
1311	1317	0.5	−3.4	?(1320)	983			HCCH symmetrical deformation
1381	1394	0.9	−3.0	1376	1379	0.2	−3.7	CH_3 symmetrical deformation
1449	1455	0.0	−3.7	1447	1450	0.2	−3.8	CH_3 antisymmetric deformation
1453	1445	0.1	−4.1	1450	1453	0.2	−3.7	CH_3 antisymmetric deformation
1640	1709	4.2	−0.2	1631	1698	4.1	0.0	C=C stretch
2232	2337	4.7	0.7	2230	2334	4.7	0.6	C≡N strecth
2932	3022	3.1	−0.9	2922	3024	4.6	−0.5	CH_3 symmetric stretch
2965	3077	3.8	−0.2	2952	3078	4.3	0.2	CH_3 antisymmetric stretch
2987	3119	4.4	0.4	2972	3130	5.3	1.2	CH_3 antisymmetric stretch
3036	3158	4.0	0.0	3052[f]	3158	3.5	−0.5	HCCH symmetrical strech
3060	3167	3.5	−0.5	3070	3187	3.8	−0.2	HCCH symmetrical strech

[a] Experimental frequencies observed in the infrared spectrum of the gas unless noted as *d* and *f*. [b] Δ = (calculated value − experimental value)/experimental value, in percent. [c] Scaling factor is 0.9613.[30] [d] Mode description from ref 31. [e] Far-infrared spectrum of solid. [f] Raman spectrum of liquid.

TS1 is a disrotatory motion of the terminal methylene group with respect to central methylene group and conrotatory motion of the H−C−CN group with respect to central methylene group. In TS1 the C(2)−C(3) bond is practically ruptured; it is 2.52 Å compared to 1.52 Å in cyclopropanecarbonitrile. Also, the angle C(2)C(1)C(3) becomes ∼114° compared to 59° in the reactant. Some pyramidalization of the central methylene group H(1)-C(1)H(2) in TS1 takes place, which expresses itself by change in the angles H(1)C(1)C(2), H(1)C(1)C(3), H(2)C(1)C(2), and H(2)C(1)C(3) from ∼118° in cyclopropanecarbonitrile to the tetrahedral value of ∼108−110°. Some shortening of the remaining carbon−carbon bonds is observed. The most pronounced shortening is associated with the C−CN bond. All of these changes are much more pronounced in the intermediate INT1 than in TS1 (Tables 8 and 9). The optimized structure of the intermediate has a cis conformation. An attempt to localize a trans conformer of the intermediate was unsuccessful despite many trials using both uB3LYP and TCSCF methods.

TABLE 4: Structural Parameters of Cyclopropanecarbonitrile and Its Isomerization Products Calculated at the B3LYP Level of Theory

parameter[a]	CPRN	*cis*-CRNT	*trans*-CRNT	VACN	MACN
r-C(1)C(2)[b]	1.501	1.495	1.495	1.334	2.627
r-C(1)C(3)	1.524	1.346	1.345	1.514	1.509
r-C(2)C(3)	1.524	2.534	2.515	2.539	1.343
r-C(3)C(4)	1.443	1.432	1.431	1.466	1.443
r-C(4)N	1.163	1.165	1.164	1.162	1.164
∠C(2)C(1)C(3)	59.0	126.3	124.6	126.0	
∠C(1)C(3)C(2)	60.5				134.4
r-H(1)C(1)	1.092	1.096	1.096	2.158	
r-H(2)C(1)	1.091	2.145	2.148	1.095	
r-H(2)C(2)	2.241	1.099	1.100	2.109	
r-H(1)C(3)	2.240	2.085	2.101	1.105	
r-H(5)C(1)					2.162
r-H(5)C(3)	1.093				1.102
∠H(1)C(1)C(2)	118.8			116.8	
∠H(1)C(1)C(3)	116.4			116.9	
∠H(2)C(1)C(2)	118.2	116.8	117.0		
∠H(2)C(1)C(3)	117.3	116.9	118.4		
τH(3)C(2)C(1)C(3)	−106.8	121.4	121.2	0.0	
τH(4)C(2)C(1)C(3)	105.8	0.0	0.0	180.0	
τH(5)C(3)C(1)C(2)	−106.9	0.0	0.0	−122.0	
τC(4)C(3)C(1)C(2)	108.6	180.0	180.0	0.0	
τH(3)C(2)C(3)C(1)	−109.6				180.0
τH(4)C(2)C(3)C(1)	108.7				0.1
τH(1)C(1)C(3)C(2)	108.7				120.6
τH(2)C(1)C(3)C(2)	109.6				0.0
τH(1)C(1)C(3)H(5)	−2.7	0.0	180.0		

[a] Distances in angstroms, angles in degrees. [b] Atom numbers are shown in Figures 2-4.

TABLE 5: B3LYP/cc-pVDZ Frequencies (cm^{-1}) of the Vinylacetonitrile and Methacrylonitrile[a]

VACN	148, 162, 371, 400, 565, 625, 876, 946, 962, 964, 1021, 1085, 1222, 1314, 1342, 1424, 1434, 1723, 2365, 3023, 3052, 3143, 3159, 3241
MACN	181, 194, 292, 387, 557, 593, 751, 771, 956, 965, 1023, 1061, 1285, 1395, 1421, 1446, 1464, 1695, 2336, 3035, 3099, 3133, 3153, 3255

[a] Experimental values are unavailable.

TABLE 6: B3LYP/cc-pVDZ Molecular Parameters of Cyclopropanecarbonitrile and Its Isomerization Products

	moments of inertia[a]					
	$A \times 10^{38}$	$B \times 10^{37}$	$C \times 10^{37}$	μ[b]	S[c]	ZPE[d]
CPRN	5.2966	2.4588	2.5939	4.05	69.987	50.11
c-CRNT	6.9564	2.4588	3.1022	4.03	73.324	49.37
t-CRNT	2.1916	3.6904	3.8573	4.49	73.205	49.22
VACN	7.3386	2.3082	2.9901	3.61	72.899	49.42
MACN	9.0898	2.0269	2.8833	3.74	72.934	49.24

[a] Moments of inertia in g·cm^2. [b] Dipole moments in D. [c] Entropy in cal/(K·mol). [d] Zero-point energy in kcal/mol.

The second stage in the biradical manifold is the formation of the three main products from the biradical intermediate as shown in Figures 3 and 4. The geometrical parameters of the transition states leading to these products are shown in Tables 8 and 9. All the transition state (TS2−TS5) have the edge-to-edge (EE, or "0,0") structure of a CN-substituted trimethylene. There are two transition states leading to the formation of vinylacetonitrile that have very similar energetics (Table 11). They differ, however, in the spatial structure, namely, cis and gauche configuration. These two transition states lead to the production of vinylacetonitrile as is shown in Figure 4. Since the barrier between these two conformers is very small,[32] they are kinetically indistinguishable.

The reaction coordinate in the transition states TS2−TS4 is a combination of two normal modes. They are 1,2-H atom shift

TABLE 7: Total Energies E_{total} (in au) and Relative Energies ΔE_{total} and ΔE[a] (in kcal/mol) of the Reactant and Its Isomerization Products at B3LYP and QCISD(T) Computational Levels

	B3LYP			QCISDT		
	E_{total}	ΔE_{total}	ΔE	E_{total}	ΔE_{total}	ΔE
CPRN	−210.147 473	0.00	0.00	−209.561 956	0.00	0.00
c-CRNT	−210.164 877	−10.92	−11.66	−209.577 508	−9.76	−10.50
t-CRNT	−210.164 652	−10.78	−11.67	−209.577 213	−9.57	−10.46
VACN	−210.155 474	−5.02	−5.75	−209.570 771	−5.53	−6.22
MACN	−210.162 141	−9.20	−10.07	−209.576 008	−8.82	−9.69

[a] $\Delta E = \Delta E_{total} + \Delta$(ZPE).

of H(2) from the central carbon atom C(1) to C(2) in TS2 and TS3, and of H(1) to C(3) in TS3 and TS4, as well as an asymmetric stretch of C(2)C(1)C(3). The frequencies, including the imaginary ones, of all the biradical species are shown in Table 10. The distances C(1)−H(2) in TS2 and TS3 and C(1)−H(1) in TS4 and TS5 become longer (∼1.18 Å in comparison with 1.11 Å in the intermediate INT1), and the distances C(2)−H(2) in TS2 and TS3 and C(3)−H(1) in TS4 and TS5 become shorter (1.58−1.64 Å in comparison with 2.12−2.14 Å in the intermediate INT1). The angles C(2)C(1)C(3) widen from 118° in the intermediate to about 127° in the transition states TS2−TS4. The relative distances of C(1)−C(2) and C(1)−C(3) in the transition states show which bond will become a double or a single bond in the products (Tables 8 and 9).

B. The Electronic Characteristics of the Transition States TS1−TS5 and the Intermediate INT1. The calculations, both at uB3LYP and TCSCF level of theory, clearly indicate that the transition state TS1 and the intermediate have a much higher biradical character than the transition states leading from the intermediate to the products. These transition states are mainly closed shell singlet with some biradical character. The wave functions obtained by the TCSCF calculations of all the trimethylene cyanide conformers, namely, the transition states and the intermediate, are as follows: 110 = 0.898, 200 = 0.113 in TS1, 110 = 0.877, 200 = 0.114 in INT1, 110 = 0.702, 200 = 0.648 in TS2, 110 = 868, 200 = 460 in TS3, 110 = 0.825, 200 = 0.549 in TS4, and 110 = 0.809, 200 = 0.547 in TS5. The three digits 110 are the configuration of the single occupied orbital with α spin, the single occupied orbital with β spin, and the vacant orbital, respectively. The three digits 200 are the configuration of the double occupied orbital, nonoccupied orbital, and the vacant orbital, respectively. The electron occupation numbers of the orbitals are 1.30 and 0.70 in TS1, 1.13 and 0.87 in INT1, 1.66 and 0.34 in TS2 and TS3, 1.68 and 0.32 in TS4, and 1.67 and 0.33 in TS5.

We have also estimated qualitatively the biradical character χ of the various trimethylene cyanide conformers according to the method of Kraka and Cremer.[33] In this method the expression for χ is given by $\chi = \Sigma\eta_i - \Sigma\eta_i$(ref), where, for a system with 2*n* electrons, $\Sigma\eta_i$ is the sum over all occupation numbers of the natural orbitals η_i, where $i > n$. $\Sigma\eta_i$(ref) is the sum over all occupation numbers of the natural orbitals in a reference molecule, e.g., cyclopropanecarbonitrile in our case. We used this expression for uB3LYP and TCSCF calculations, by which the wave functions were obtained. Both methods show the same results namely, considerably higher biradical character of TS1 and the intermediate INT1 compared to TS2−TS5.

A similar behavior was observed in cyclopropane isomerizations.[25] The geometrical and optical isomerizations that involve no H-atom shift have transition states and intermediate with considerably high biradical character. The electron oc-

TABLE 8: Structural Parameters of C_3H_5CN Biradical Species at the uB3LYP Level of Theory

parameter[a]	TS1	INT1	TS2	TS3	TS4	TS5	TS6	TS7
r-C(1)C(2)[b]	1.493	1.485	1.466	1.468	1.408	1.411	2.612	1.484
r-C(1)C(3)	1.505	1.497	1.436	1.432	1.490	1.486	1.496	1.440
r-C(2)C(3)	2.516	2.562	2.598	2.594	2.601	2.593	1.432	2.593
r-C(3)C(4)	1.394	1.389	1.402	1.403	1.402	1.403	1.461	1.397
r-C(4)N	1.177	1.178	1.174	1.173	1.173	1.172	1.162	1.178
∠C(2)C(1)C(3)	114.2	118.4	127.1	126.9	127.6	127.0		124.9
∠C(1)C(3)C(2)							126.2	
r-H(1)C(1)	1.110	1.114	1.097	1.097	1.194	1.195		1.103
r-H(2)C(1)	1.108	1.114	1.179	1.181	1.096	1.096		
r-H(2)C(2)	2.149	2.138	1.642	1.632	2.145	2.146		1.108
r-H(1)C(3)	2.122	2.117	2.142	2.145	1.586	1.588		
r-H(5)C(1)							1.629	
r-H(5)C(3)							1.184	1.099
∠H(1)C(1)C(2)	110.5	109.9	115.1	115.0	107.0	106.4		115.8
∠H(1)C(1)C(3)	107.6	107.5	114.8	115.4	71.5	71.7		119.3
∠H(2)C(1)C(2)	110.1	109.9	75.9	75.2	117.3	117.2		
∠H(2)C(1)C(3)	109.2	107.5	107.4	106.8	113.2	114.0		
∠H(5)C(3)C(1)							73.8	
∠H(5)C(3)C(2)							107.9	
τH(3)C(2)C(1)C(3)	−43.4	−0.1	−16.1	−16.1	−10.1	−10.0		−114.1
τH(4)C(2)C(1)C(3)	132.9	179.9	178.9	179.5	176.1	178.4		7.2
τH(5)C(3)C(1)C(2)	−139.5	179.9	−174.9	12.8	178.6	12.4		−90.6
τC(4)C(3)C(1)C(2)	40.9	0.0	−10.7	172.3	−8.0	−173.2		91.4
τH(3)C(2)C(3)C(1)							7.5	
τH(4)C(2)C(3)C(1)							172.4	
τH(1)C(1)C(3)C(2)							19.7	
τH(2)C(1)C(3)C(2)							−178.5	
τH(1)C(1)C(3)H(5)								88.9

[a] Distances in angstroms, angles in degrees. [b] Atom numbers are shown in Figures 2−6.

TABLE 9: Structural Parameters of C_3H_5CN Biradical Species at the TCSCF Level of Theory

parameter[a]	TS1	INT1	TS2	TS3	TS4	TS5	TS6	TS7
r-C(1)C(2)[b]	1.498	1.499	1.470	1.470	1.405	1.406	2.605	1.502
r-C(1)C(3)	1.503	1.503	1.414	1.412	1.476	1.474	1.489	1.480
r-C(2)C(3)	2.558	2.567	2.596	2.584	2.593	2.589	1.414	2.589
r-C(3)C(4)	1.422	1.423	1.427	1.426	1.423	1.423	1.462	1.428
r-C(4)N	1.141	1.141	1.141	1.141	1.141	1.141	1.136	1.140
∠C(2)C(1)C(3)	116.9	117.6	128.4	127.4	128.3	127.1		120.5
∠C(1)C(3)C(2)							127.7	
r-H(1)C(1)	1.098	1.099	1.084	1.084	1.198	1.198		1.085
r-H(2)C(1)	1.096	1.095	1.180	1.183	1.083	1.084		
r-H(2)C(2)	2.132	2.133	1.547	1.539	2.133	2.134		1.096
r-H(1)C(3)	2.109	2.105	2.115	2.125	1.499	1.500		
r-H(5)C(1)							1.504	
r-H(5)C(3)							1.189	1.081
∠H(1)C(1)C(2)	109.6	109.0	114.8	114.8	107.3	106.5		118.9
∠H(1)C(1)C(3)	107.2	107.0	115.1	116.2	67.3	67.4		117.0
∠H(2)C(1)C(2)	109.5	109.7	70.5	70.0	117.4	117.4		
∠H(2)C(1)C(3)	107.2	107.8	106.5	106.1	113.1	114.3		
∠H(5)C(3)C(1)							67.3	
∠H(5)C(3)C(2)							108.4	
τH(3)C(2)C(1)C(3)	−30.9	−25.9	−16.5	−16.3	9.5	9.8		−74.4
τH(4)C(2)C(1)C(3)	170.8	177.7	174.9	174.4	−179.8	178.5		168.9
τH(5)C(3)C(1)C(2)	−171.5	175.1	173.6	12.3	176.5	−8.7		−101.7
τC(4)C(3)C(1)C(2)	11.1	13.0	12.4	173.9	−6.5	174.1		78.3
τH(3)C(2)C(3)C(1)							15.1	
τH(4)C(2)C(3)C(1)							174.9	
τH(1)C(1)C(3)C(2)							17.4	
τH(2)C(1)C(3)C(2)							−175.2	
τH(1)C(1)C(3)H(5)								100.0

[a] Distances in angstroms, angles in degrees. [b] Atom numbers are shown in Figures 2−6.

cupation numbers in the transition state were approximately 1.11 and 0.89, and the degree of biradical character χ was 0.85, and 1.10 and 0.90, with $\chi = 0.87$ in the intermediate. On the other hand, the transition state of the structural isomerization of cyclopropane (cyclopropane → propylene) is a closed shell singlet with only small biradical character. The electron occupation numbers were 1.61 and 0.39, and the degree of biradical character χ was 0.27. It should be mentioned that the entire C_3H_5CN manifold shows a smaller degree of biradical character than the C_3H_6 manifold. Obviously, this is the result of the effect of the CN group. These findings are in accord with the analysis of atomic spin density distribution, as obtained at uB3LYP level of theory (Table 13). The presence of the CN group in the intermediate and in the transition states reduces the electron density on C(3) and increases the density on C(4) and on the nitrogen atom. This behavior introduces two changes

TABLE 10: uB3LYP/cc-pVDZ Frequencies of the Biradical C_3H_5CN Species (in cm^{-1})[a]

TS1	123, (**i-124**), 193, 340, 419, 481, 538, 634, 786, 877, 1025, 1056, 1149, 1207, 1307, 1363, 1403, 1441, 2158, 2968, 3000, 3149, 3179, 3266
INT1	77, 153, 154, 373, 424, 452, 556, 624, 793, 862, 973, 1075, 1131, 1163, 1334, 1360, 1393, 1443, 2145, 2937, 2938, 3153, 3186, 3269
TS2	137, 204, 395, 453, 548, 562, 646, 670, 828, 913, 997, 1100, 1210, 1243, 1372, (**i-1375**), 1431, 1483, 2232, 2461, 3134, 3158, 3215, 3283
TS3	132, 173, 384, 449, 510, 559, 641, 655, 810, 897, 1081, 1132, 1222, 1242, 1291, (**i-1388**), 1431, 1519, 2240, 2441, 3136, 3155, 3179, 3279
TS4	138, 231, 391, 452, 537, 563, 640, 686, 806, 892, 1012, 1117, 1216, 1258, 1349, 1413, 1516, (**i-1552**), 2243, 2371, 3145, 3161, 3222, 3275
TS5	148, 172, 382, 450, 510, 553, 629, 682, 796, 886, 1081, 1143, 1222, 1246, 1286, 1435, (**i-1514**), 1528, 2248, 2366, 3143, 3157, 3192, 3270
TS6	195, 280, 297, 364, 502, 542, 554, 587, 681, 777, 949, 958, 1054, 1271, 1342, (**i-1416**), 1420, 1461, 2358, 2377, 3160, 3165, 3287, 3292
TS7	85, 142, 243, 353, 560, 616, 898, (**i-948**), 958, 1019, 1087, 1182, 1299, 1376, 1413, 1433, 1470, 2140, 2952, 3006, 3060, 3091, 3134

[a] Imaginary frequencies are shown in parentheses.

when compared to cyclopropanecarbonitrile: (1) decreasing the biradical character of both transition states and intermediate and (2) shortening of the C−CN bond (∼1.40 Å in comparison with 1.44 Å in cyclopropanecarbonitrile). An additional support for the effect of the CN group can be found in the properties of TS6, which leads to the formation of methacrylonitrile. In this isomerization channel the broken bond is the C(1)−C(2) bond, which is opposite to the CN group (Figure 5). Since the CN group, is this case, in not bound to a carbon with unpaired electrons, no influence on the electron density of the carbon atoms with unpaired electron in TS6 can exist. As can be seen in Table 13 the spin densities on C(1) and C(2) are practically the same, and there is almost no spin density on C(4) and on the nitrogen atom. The electron densities on the latter are roughly the same as those on the hydrogen atoms.

C. Structure and Electronic Characteristics of the Critical Point along the Pathway of Methacrylonitrile Formation. In view of the fact that the formation of methacrylonitrile involves the cleavage of the C−C bond opposite to the CN group, there is a resemblance between the transition TS6 and the transition state of the structural isomerization of cyclopropane. This expresses itself both in the configuration of the transition state and in the reaction pathway. These two processes proceed without biradical intermediates. IRC analysis of the transition state TS6 shows that it leads to cyclopropanecarbonitrile at one end and to methacrylonitrile at the other end without the involvement of an intermediate (Figure 5), similar to what has been obtained in the calculations of the structural isomerization of cyclopropane.

The reaction coordinate in TS6 is a combination of two normal modes: 1,2 H-atom shift and an asymmetric stretch of the carbon ring. In general, the structural parameters of TS6 (Tables 8 and 9) are similar to those of the transition states TS2−TS5. There is however one main difference. Contrary to the stretch of the C−CN bond in TS1−TS5 relative to cyclopropanecarbonitrile this bond in TS6 is shorter than in the reactant. The wave function characteristics of TS6 are also similar to those of the transition states TS2−TS5 when the electron occupation numbers (1.72 and 0.28) and the biradical character ($\chi = 0.33$) are concerned. The wave function obtained by the TCSCF calculation of TS6 give the values of $110 = 0.724$, $200 = 0.535$.

The question that arises is why the transition states TS2−TS6 in which one of the C−C bonds is completely ruptured have such a small contribution of a biradical configuration. This can be attributed to two phenomena: (1) a H-atom shift and formation of a new C−H σ-bond and formation of a π-bond between two carbon atoms already at the early stages of the processes; this can be seen in the electron density distribution of the two single occupied orbitals; (2) the relatively large dipole moments of TS2−TS5 (Table 12) as compared to those of TS1, TS6 and of the intermediate INT1 indicate a high ionic character of these transition states. As a matter of fact, the relative differences are in the dipole moment of these two groups of transition states are higher than what is reflected from the table, since the dipole moment of the C≡N group is already 3.5 D.[34]

D. Energetic Characteristics of the Biradical Pathways of Cyclopropanecarbonitrile Isomerizations. There is a very little difference between the energy of the transition state of the ring-opening TS1 and the energy of the short-lived trimethylene cyanide intermediate. Such a shallow potential energy surface in the region of the biradical intermediate was obtained also in cyclopropane isomerization. This is characteristic of small ring rearrangements.[16,35,36] Thus, the inverse cyclization of the intermediate has very little or no barrier, and its lifetime is determined by entropy considerations rather than by energy. The existence of such short-lived intermediate does not affect at all the kinetic characteristics of the product formation.

The calculated relative energies of the intermediate INT1 and the transition states TS1−TS6, at uB3LYP/cc-pVDZ, uQCISD(T)//B3LYP/cc-pVDZ, and TCSCF/cc-pVDZ levels of theory with ZPE correction are shown in Table 11. Note that the energy level of TS6, the transition state that leads to the formation of methacrylonitrile, is higher than those of TS2−TS5 by approximately 10 kcal/mol. As has been mentioned before, this is the result of a lack of stabilization of TS6 in comparison with the other transition states, in view of the large distance of the CN group from the carbon atoms with the unpaired electrons. This finding is supported also by the very minute quantities of methacrylonitrile found experimentally in the isomerization of cyclopropanecarbonitrile.

V. Interisomerizations among the Reaction Products

We have examined also the possibility of interisomerizations among the reaction products via a biradical mechanism. We found, using the uB3LYP method, only one additional transition state (TS7) describing the cis−trans isomerization of crotonitrile. The route leading from vinylacetonitrile to either *cis*- or *trans*-crotonitrile proceeds via the intermediate INT1 as was proposed earlier.[37] Cis−trans isomerization is associated with a bond rupture so that the transition state must be biradical. There are in principle two mechanisms: the molecule remains in the singlet state throughout, or alternatively, the molecule undergoes intersystem crossing to the lowest triplet state.[38] We used in our calculations only the singlet biradical path. The optimized structure of the transition state TS7 of the cis−trans isomerization of crotonitrile is shown in Figure 6. It is a gauche-conformer of crotonitrile with a broken C(1)−C(3) π-bond. It extends from 1.35 Å in *cis*- and *trans*-crotonitrile to 1.44 Å in TS7. Also, a considerable shortening of the C−CN bond takes place (Tables 8 and 9). Such shortening hints to a strong influence of the CN group. In contradiction to the other biradical species, TS7 is a 1,2-biradical with $\chi = 1.0$ rather than a 1,3-biradical (Tables 12 and 13). The reaction coordinate is the torsional motion around the C(1)−C(3) bond (Figure 6).

TABLE 11: Calculated Total Energies E_{total} (in au) and Relative Energies ΔE_{total} and $\Delta E^{\ddagger}$ [a] (in kcal/mol) of All the C_3H_5CN Biradical Species at Different Computational Levels

	uB3LYP			uQCISDT			TCSCF		
	E_{total}	ΔE_{total}	$\Delta E^{\ddagger}$	E_{total}	ΔE_{total}	$\Delta E^{\ddagger}$	E_{total}	ΔE_{total}	$\Delta E^{\ddagger}$
CPRN	−210.147 473	0.00	0.00	−209.561 956	0.00	0.00	−208.831 579	0.00	0.00
TS1	−210.067 551	50.15	45.87	−209.475 230	54.42	50.14	−208.749 698	51.39	46.92
INT1	−210.068 608	49.48	45.07	−209.475 474	54.26	49.85	−208.749 725	51.37	47.20
TS2	−210.053 640	58.88	54.05	−209.461 272	63.18	58.35	−208.724 772	67.02	61.88
TS3	−210.052 177	59.79	54.80	−209.459 469	64.31	59.32	−208.723 340	67.92	62.57
TS4	−210.049 292	61.60	56.71	−209.457 623	65.45	60.56	−208.720 656	69.61	64.51
TS5	−210.048 284	62.20	57.16	−209.456 166	66.38	61.34	−208.719 822	70.13	64.67
TS6	−210.028 404	74.71	69.35	−209.442 784	74.78	70.42	−208.708 727	77.09	70.89
TS7[b]	−210.071 651	58.50	54.80	−209.477 435	62.80	59.10	−208.752 717	65.20	62.28

[a] $\Delta E^{\ddagger} = \Delta E_{total} + \Delta(ZPE)$. [b] Relative energy for TS7 is obtained with respect to *cis*-crotonitrile.

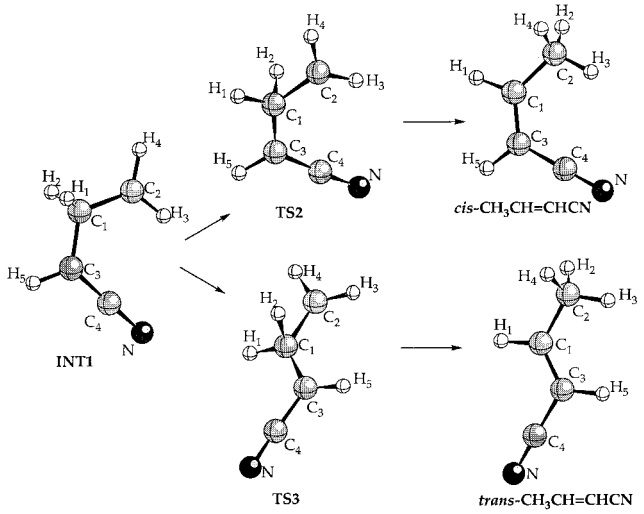

Figure 3. Formation of *cis*- and *trans*-crotonitrile from the intermediate INT1 via the transition states TS2 and TS3.

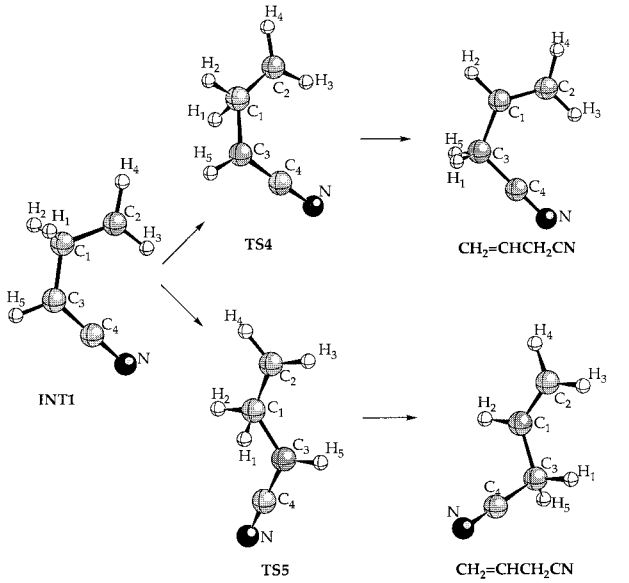

Figure 4. Formation of two conformers of vinylacetonitrile from the intermediate INT1 via the transition states TS4 and TS5.

It should be mentioned that at the TCSCF level of theory and also at a complete active space multiconfiguration self-consistent-field CASSCF with 4,4-CAS wave functions we could only localize a second-order stationary point with a structure very similar to TS7. One of the imaginary frequencies of this structure was that of the torsional motion around the C(1)−C(3) bond as was found in TS7 with the uB3LYP calculations. The second imaginary frequency is a rotation of methyl group with respect to C(1)−C(2) bond.

TABLE 12: Molecular Parameters of Biradical C_3H_5CN Species Calculated Using Two Different Computational Methods

	momemts of inertia[a]							
	$A \times 10^{38}$	$B \times 10^{37}$	$C \times 10^{37}$	μ[b]	S[c]	ZPE[d]	χ[e]	$\langle S^2\rangle$[f]
				uB3LYP/cc-pVDZ				
TS1	7.1267	2.5246	3.0695	3.81	73.770	45.83	0.77	0.9624
INT1	7.1771	2.5704	3.0982	3.94	77.655	45.70	0.80	0.9767
TS2	6.9274	2.4578	3.1020	4.94	73.087	45.28	0.24	0.4214
TS3	2.4014	3.6357	3.8258	5.38	73.177	45.12	0.24	0.4278
TS4	6.7402	2.5165	3.1452	4.43	72.897	45.22	0.20	0.3538
TS5	2.4480	3.6164	3.8115	4.22	72.981	45.07	0.21	0.3730
TS6	9.3756	2.0022	2.8796	3.65	73.424	45.75	0.33	0.5566
TS7	5.1860	3.1315	3.3917	3.76	75.902	45.67	1.00	1.0230
				TCSCF/cc-pVDZ				
TS1	7.1886	2.4477	3.0976	4.31	72.671	49.20	0.84	
INT1	7.1666	2.4477	3.1072	4.22	75.435	49.50	0.84	
TS2	6.8072	2.4563	3.0908	4.91	71.803	48.53	0.21	
TS3	2.3524	3.6024	3.7926	5.48	71.368	48.32	0.22	
TS4	6.6489	2.4978	3.1204	4.57	71.744	48.57	0.22	
TS5	2.4354	3.5660	3.7643	4.44	71.809	48.21	0.23	
TS6	9.2701	1.9648	2.8430	4.07	71.781	47.47	0.26	
TS7	5.8031	2.9995	3.3253	3.86	71.395	49.51	0.98	

[a] Moments of inertia in g·cm^2. [b] Dipole moments in D. [c] Entropy in cal/(K·mol). [d] Zero-point energy in kcal/mol. [e] Biradical character in %. As it was proposed in ref 33, we have defined the biradical character χ by $[\Sigma\eta_i - \Sigma\eta_i(\text{ref})]$, where cyclopropanecarbonitrile has been taken as a reference molecule. For a system with $2n$ electrons, $\Sigma\eta_i$ is defined as a sum over all occupation numbers for natural orbitals η_i with $i > n$. [f] Spin contamination at the uB3LYP level of theory.

VI. Nonradical Mechanisms of Cyclopropanecarbonitrile Isomerization

In addition to the biradical mechanism, we examined the possibility of the existence of a concerted (nonradical) mechanism for the isomerization of cyclopropanecarbonitrile and for the interisomerization of the products. Using the B3LYP method we were able to localize three nonradical transition states TS8−TS10 leading directly from cyclopropanecarbonitrile to *cis*- and *trans*-crotonitrile and vinylacetonitrile, without the involvement of an intermediate. We also localized transition states TS11 and TS12 corresponding to the interisomerization *cis*-crotonitrile → vinylacetonitrile and *trans*-crotonitrile → vinylacetonitrile, respectively. Figure 7 shows the structures of TS10 and TS11 as examples of these nonradical transition states. To our surprise, the structures of these transition states were not compatible at all with the expected structures of nonradical transition states. This expressed itself by the very long (∼2.52 Å), completely broken C(2)−C(3) bonds similar

TABLE 13: Atomic Spin Densities of Biradical Species of Trimethylenecyanide at the uB3LYP/cc-pVDZ Level[a]

	C(1)	C(2)	C(3)	C(4)	N	H(1)	H(2)	H(3)	H(4)	H(5)
TS1	−0.01	1.02	−0.78	0.19	−0.38	−0.04	0.04	−0.04	−0.04	0.04
INT1	−0.01	1.05	−0.77	0.19	−0.40	0.00	0.00	−0.04	−0.04	0.04
TS2	0.07	0.63	−0.47	0.11	−0.22	0.00	−0.08	−0.02	−0.02	0.02
TS3	0.07	0.63	−0.49	0.11	−0.22	−0.00	−0.08	−0.02	−0.02	0.02
TS4	−0.11	0.59	−0.42	0.10	−0.21	0.06	0.00	−0.02	−0.02	0.02
TS5	−0.11	0.61	−0.44	0.10	−0.21	0.07	0.00	−0.02	−0.02	0.02
TS6	−0.72	0.75	−0.11	0.02	−0.03	0.03	0.03	−0.03	−0.03	0.09
TS7	1.03	−0.07	−0.86	0.22	−0.38	−0.08	0.04	0.05	0.00	0.08

[a] Positive number indicates an excess α-spin occupancy. negative number indicates an excess β-spin occupancy.

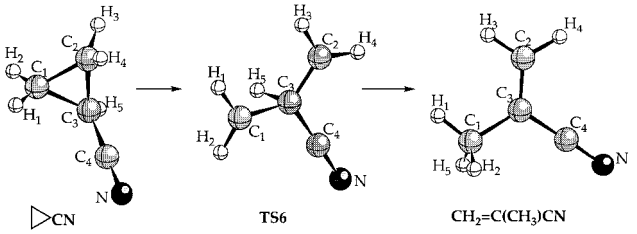

Figure 5. Formation of methacrylonitrile from cyclopropanecarbonitrile via the transition state TS6. This is a concerted pathway with a small biradical character.

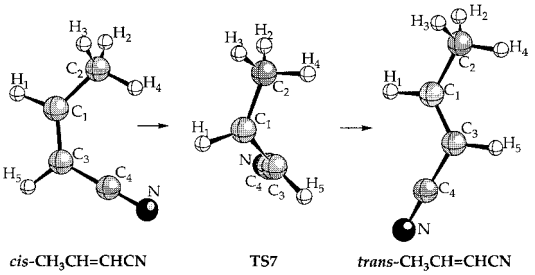

Figure 6. Cis−trans isomerization of crotonitrile via the transition state TS7. This transition state is a biradical with $\chi = 1$ (see text).

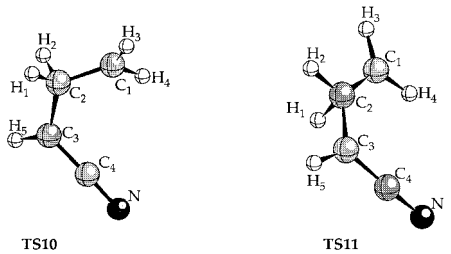

Figure 7. Transition states TS10 and TS11 of concerted closed shell singlet structures. The transition states of the closed shell manifold show Hartree−Fock instability and intersystem cross to the biradical manifold.

to the equivalent distance in TS1 without any indication of a new bond formation. Moreover, although a bond is broken, there is no dipole moment to indicate the existence of a zwitterionic character. The B3LYP/cc-pVDZ and QCISD(T)//B3LYP/cc-pVDZ energies of TS8-TS10 are very similar to those of TS2−TS5. We could not explain the above-mentioned discrepancy and therefore examined whether there were Hartree−Fock instabilities in the wave functions describing the transitions states TS8−TS10. Indeed, we found such instabilities in the wave functions. To clarify this point the wave functions of TS8−TS12 were reoptimized with appropriate reduction in constraints, followed by the geometrical optimization using the uB3LYP method. The optimization starting from the transition states TS8−TS10 led to the biradical ring-opening transition state TS1. The optimization starting from the transition states of the product interisomerizations TS11 and TS12 led to the transition states TS4 and TS5 of vinylacetonitrile formation from the biradical intermediate INT1, respectively. Optimization of the geometry of the closed shell transition states TS8−TS12 performed by the TCSCF method gave the same results. The optimization did not lead to any new transition state. This behavior hints of the possibility of an intersystem crossing from the nonradical closed shell potential energy surface to that of the open shell biradical singlet manifold. The existence of a real nonradical concerted mechanism in the C_3H_5-CN manifold is thus very questionable.

VII. Comparison with the Experiment−Kinetic Modeling

The isomerization of cyclopropanecarbonitrile was studied experimentally both at low[13] and at high temperatures.[14] It is of interest now to compare the results of the quantum chemical calculations to the experimental rates. For this purpose we calculated high-pressure limit rate constants from the calculated parameters of the reactant and the transition states, performed RRKM calculations to transfer the high-pressure limit rate constants to the experimental conditions, and then ran computer modeling of all the reactions involved and compared the results to the experiment.

The Arrhenius rate parameters for the unimolecular isomerizations were calculated using the expression:[39,40] $k_\infty = \sigma(kT/h)\exp(\Delta S^\ddagger/R)\exp(-\Delta H^\ddagger/RT)$, where h is the Planck constant, k is the Boltzmann constant, σ is the degeneracy of the reactional coordinate, and $\Delta H^\ddagger$ and $\Delta S^\ddagger$ are the enthalpy and entropy of activation respectively. Values of σ for each reaction are given in Table 14. Since we deal with isomerizations where there is no change in the number of moles, then $\Delta H^\ddagger = \Delta E^\ddagger$, where $\Delta E^\ddagger$ is the energy difference between the transition state and the reactant. $\Delta E^\ddagger$ is equal to $\Delta E^0_{\text{total}} + \Delta(\text{ZPE})$, where $\Delta E^0_{\text{total}}$ is obtained by taking the difference between the total energies of the transition state and the reactant and Δ(ZPE) is the difference between ZPE of these species. Calculated entropies and zero-point energies are shown in Table 7 and total energies and $\Delta E^\ddagger$ in Table 8. For comparison with the experimental rate parameters (A and E_a), we replaced $\Delta E^\ddagger$ by E_a where $E_a = \Delta E^\ddagger + RT$ and used the relation $k_\infty = \sigma(ekT/h)\exp(\Delta S^\ddagger/R)\exp(-E_a/RT)$. A in the expression $k_\infty = A\exp(-E_a/RT)$ is given by $A = \sigma(ekT/h)\exp(\Delta S^\ddagger/\text{R})$.

At first we ran computer simulation using the calculated values of k_∞ using two reaction schemes, one containing the intermediate and one in which the reactant goes directly to the products, where E_a was obtained from the energy difference between the reactant and TS2−TS5. In view of the fact that a potential energy surface in the vicinity of the intermediate is very shallow, the two schemes gave exactly the same results. We therefore used the scheme without the intermediate and performed RRKM calculations to transfer the k_∞ values to the experimental conditions. The RRKM calculations employed the standard routine,[41] which uses a direct vibrational state count with classical rotation for the transition state. $\langle\Delta E_{\text{down}}\rangle$ was

TABLE 14: Reaction Scheme for the Isomerization of Cyclopropanecarbonitrile and of Its Product Interisomerization at 1000 K

	reaction	σ^a	$\Delta S^{\ddagger\,b}$	$A^{c,e} \times 10^{-14}$	$E_a{}^{d,e}$	$A_\infty{}^c \times 10^{-14}$	$E_\infty{}^d$	$\Delta S^\circ{}_{react}{}^{b,c}$	$\Delta H^\circ{}_{react}{}^d$
1	CPRN → *c*-CRNT	4	3.10	2.75	58.12	8.42	60.34	3.34	−10.50
2	CPRN → *t*-CRNT	4	3.19	3.63	59.44	11.30	61.31	3.22	−10.46
3	CPRN → VACN	4	2.91	3.47	61.01	9.81	62.55	2.91	−6.22
4	CPRN → VACN	4	2.99	4.58	61.91	10.19	63.33	2.91	−6.22
5	CPRN → MACN	2	3.44	3.03	71.69	6.39	72.41	2.95	−9.69
6	*c*-CRNT → *t*-CRNT	1	2.58	0.84	60.19	2.07	61.09	−0.12	0.04
7	*c*-CRNT → VACN	2	−0.24	0.48	70.60	1.01	70.84	−0.43	4.28
8	*t*-CRNT→ VACN	2	−0.03	0.53	71.60	1.12	71.77	−0.31	4.24

[a] σ is the factor of the degeneracy of the reactional coordinate. [b] Entropy of activation and entropy of reaction in cal/(K·mol). [c] Preexponential factor A in s^{-1}. [d] Activation energy and enthalpy of reaction in kcal/mol. [e] Activation energy and preexponential factors at a pressure of 1800 Torr.

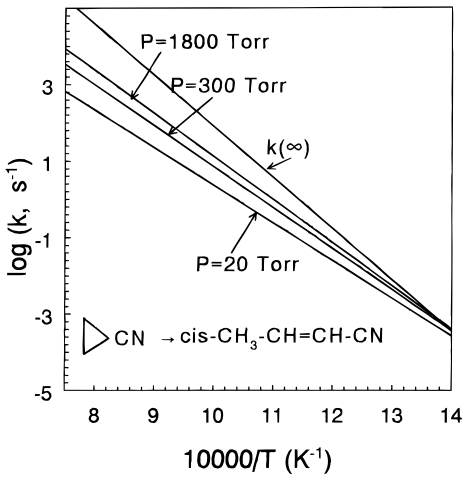

Figure 8. RRKM calculations of the first-order rate constants of the isomerization of cyclopropanecarbonitrile to *cis*-crotonitrile at different pressures. k_∞ is evaluated from the calculated $\Delta S^\ddagger$ and $\Delta E^\ddagger$ (see text). The value of k at 1800 Torr is used for the modeling.

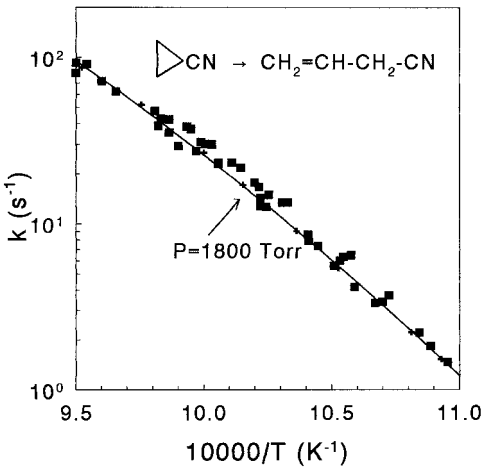

Figure 10. Isomerization cyclopropanecarbonitrile → vinylacetonitrile at 1800 Torr. The squares are experimental points taken from a recent single-pulse shock tube experiment,[14] and the solid line is the best fit to seven calculated rate constants (shown on the line as small crosses). As can be seen the agreement is very good.

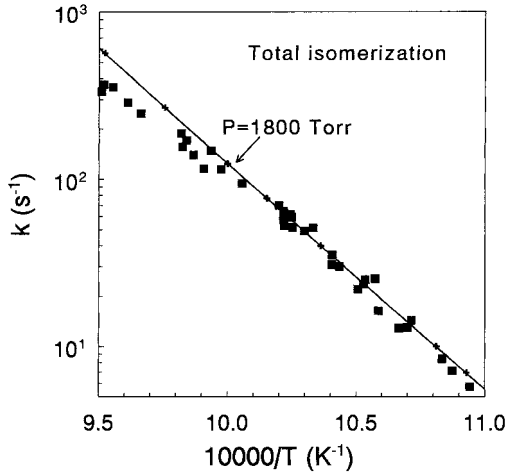

Figure 9. Total isomerization of cyclopropanecarbonitrile at 1800 Torr. The squares are experimental points taken from a recent single-pulse shock tube experiment,[14] and the solid line is the best fit to seven calculated rate constants (shown on the line as small crosses). As can be seen the agreement is very good.

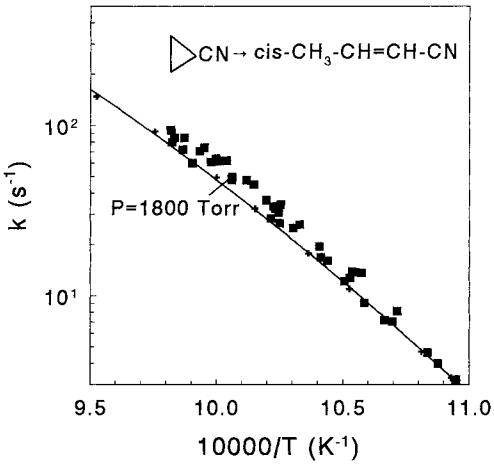

Figure 11. Isomerization cyclopropanecarbonitrile → *cis*-crotonitrile at 1800 Torr. The squares are experimental points taken from a recent single-pulse shock tube experiment,[14] and the solid line is the best fit to seven calculated rate constants (shown on the line as small crosses). The calculated line slightly underestimates the measured rate.

taken as 400 cm^{-1}. Figure 8 shows as an example of such calculation for the reaction cyclopropanecarbonitrile → *cis*-crotonitrile.

The reaction scheme containing all the reactions that participate in the overall isomerization of the biradical manifold of C_3H_5CN, the high-pressure limit Arrhenius parameters A_∞ and E_∞, and the RRKM calculated parameters at 1800 Torr are shown in Table 14. Figure 9 shows the calculated rate constant of the overall isomerization of cyclopropanecarbonitrile using the RRKM rate constant at 1800 Torr as compared to the results of a recent shock tube study of the isomerization at that pressure.[14] The squares on the figure are the experimental points, and the solid line is the best fit to seven calculated points. As can be seen the agreement is excellent. Figures 10−12 show similar Arrhenius plots of the isomerization rates to the three products. As can be seen the agreement between the calculated and the experimental rates of vinylacetonitrile formation is very

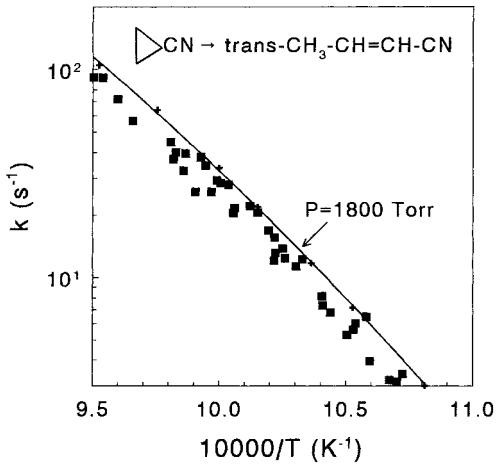

Figure 12. Isomerization cyclopropanecarbonitrile → *trans*-crotonitrile at 1800 Torr. The squares are experimental points taken from a recent single-pulse shock tube experiment,[14] and the solid line is the best fit to seven calculated rate constants (shown on the line as small crosses). The calculated line slightly overestimates the measured rate.

good. The rate of *trans*-crotonitrile formation is slightly overestimated in the calculations on the expense of the formation of the cis isomer. It should be mentioned that the interisomerization among the products, having higher activation energies, do not affect their distribution.

VIII. Conclusions

Quantum chemical calculations of cyclopropanecarbonitrile using the density functional method with a cc-pVDZ basis set reproduce well its experimental structural parameters and vibrational frequencies. This basis set and uB3LYP, uQCISD-(T), and TCSCF methods were used for calculating the different pathways of its isomerization and of the interisomerization of the products.

The calculations indicate that the isomerization of cyclopropanecarbonitrile proceeds via biradical mechanism with 1,3-biradical intermediate. The transition states and the intermediate were calculated, and their parameters and vibrational frequencies are reported. There are two types of the transition states in the biradical manifold of C_3H_5CN. The ring opening in the transition state TS1 involves merely a C−C bond rupture. It has a pyramidal type structure and a high biradical character. The transition states TS2−TS5 are associated also with H-atom shifts. They have a polar structure with low biradical configurations. The stabilizing effect of the CN group in the transition states and in the intermediate is established. Ring opening in TS6 has a higher activation barrier because of lack of stabilization of the far CN group. The formation of methacrylonitrile via TS6 is similar to the structural isomerization of cyclopropane; that is, it proceeds via a concerted mechanism with no intermediate.

Localized nonradical concerted transition states for product formation show Hartree−Fock instability. On the basis of the quantum chemical calculations, kinetic modeling of the overall isomerization was carried out. The results are in very good agreement with the experiment.

Acknowledgment. The authors thank the Ministry of Absorption for a fellowship to F.D. We also thank Dr. D. Danovich for help in providing of calculations.

References and Notes

(1) Hoffman, R. *J. Am. Chem. Soc.* **1968**, *90*, 1475.
(2) Yamaguchi, Y.; Schaefer, H. F., III; Baldwin, J. E. *Chem. Phys. Lett.* **1991**, *185*, 143.
(3) Baldwin, J. E.; Yamaguchi, Y.; Schaefer, H. F., III. *J. Phys. Chem.* **1994**, *98*, 7513.
(4) Horsley, J. A.; Jean, Y.; Moser, C.; Salem, L.; Stevens, R. M.; Wright, J. S. *J. Am. Chem. Soc.* **1972**, *94*, 279.
(5) Hay, P. J.; Hunt, W. J.; Goddard, W. A. *J. Am. Chem. Soc.* **1972**, *94*, 638.
(6) Doubleday, C., Jr.; McIver, J., Jr.; Page, M. *J. Am. Chem. Soc.* **1982**, *104*, 6533.
(7) Getty, S. S.; Davidson, E. R.; Borden, W. T. *J. Am. Chem. Soc.* **1992**, *114*, 2085.
(8) Skancke, A.; Schaad, L. J.; Hess, B. A., Jr. *J. Am. Chem. Soc.* **1988**, *110*, 5315.
(9) Laidler, K. J.; Loucks, L. F. In *Comprehensive chemical kinetics*; Bamford, C. H., Tipper, C. F. H., Eds.; Elsevier Publishing Company: Amsterdam, 1972; Vol. 5, p 1.
(10) Bergman, R. G. In *Free Radicals*; Wiley-Interscience Publishers: New York, 1973; Vol. 1, p 191.
(11) Parry, K. A.; Robinson, P. J. *J. Chem. Soc. B* **1969**, 49.
(12) Parry, K. A.; Robinson, P. J. *Int. J. Chem. Kinet.* **1973**, *5*, 27.
(13) Luckraft, D. A.; Robinson, P. J. *Int. J. Chem. Kinet.* **1973**, *5*, 137.
(14) Lifshitz, A.; Shweky, J. H.; Kiefer, J. H.; Sidhu, S. S. In *Shock Waves*; Proceeding of the 18th International Symposium on Shock Waves, Sendia, Japan, 1991, Takayama, K. Ed.; Springer-Verlag: Berlin, 1992; p 825.
(15) Doering, W. von E.; Birladeanu, L. *Tetrahedron* **1973**, *29*, 499.
(16) Doubleday, C., Jr. *J. Phys. Chem.* **1996**, *100*, 3520.
(17) Doubleday, C., Jr.; Bolton, K.; Peslherbe, G. H.; Hase, W. L. *J. Am. Chem. Soc.* **1996**, *118*, 9922.
(18) Becke, A. D. *J. Chem. Phys.* **1993**, *98*, 5648.
(19) Lee, C.; Yang, W.; Parr, R. G. *Phys. Rev.* **1988**, *B37*, 785.
(20) Frisch, M. J.; Trucks, G. W.; Schlegel, H. B.; Gill, P. M. W.; Johnson, B. G.; Robb, M. A.; Cheeseman, J. R.; Keith, T.; Petersson, G. A.; Montgomery, J. A.; Rahavachari, K.; Al-Laham, M. A.; Zakrzewski, V. G.; Orviz, J. V.; Foresman, J. B.; Cioslowski, J.; Stefanov, B. B.; Nanayakkara, A.; Challacombe, M.; Peng, C. Y.; Ayala, P. Y.; Chen, W.; Wong, M. W.; Andres, J. L.; Replogle, E. S.; R. Gomperts, R.; Martin, R. L.; Fox, D. J.; Binkley, J. S.; Defrees, D. J.; Baker, J.; Stewart, J. P.; Head-Gordon, M.; Gonzalez, C.; Pople, J. A. *GAUSSIAN94*, Revision B.1; Gaussian, Inc.: Pittsburgh, PA, 1995.
(21) Hehre, W. J.; Detchfield, R. D.; Pople, J. A. *J. Chem. Phys.* **1972**, *56*, 2257.
(22) Dunning, T. H., Jr. *J. Chem. Phys.* **1989**, *90*, 107.
(23) Kendall, R. A.; Dunning, T. H. Jr.; Harrison, R. J. *J. Chem. Phys.* **1992**, *96*, 6796.
(24) Pople, J. A.; Head-Gordon, M.; Raghavachari, K. *J. Chem. Phys.* **1987**, *87*, 5968.
(25) Dubnikova, F.; Lifshitz, A. *J. Phys. Chem. A* **1998**, *102*, 3299.
(26) Schmidt, M. W.; Baldridge, K. K.; Boatz, J. A.; Elbert, S. T.; Gordon, M. S.; Jensen, J. H.; Koseki, S.; Matsunaga, N.; Nguyen, K. A.; Su, S. J.; Windus, T. L.; Dupuis, M.; Montgomery, J. A. *GAMESS-USA*, Revision Mar. 1997; See, e.g.: Schmidt, M. W.; Baldridge, K. K.; Boatz, J. A.; Elbert, S. T.; Gordon, M. S.; Jensen, J. H.; Koseki, S.; Matsunaga, N.; Nguyen, K. A.; Su, S. J.; Windus, T. L.; Dupuis, M.; Montgomery, J. A. *J. Comput. Chem.* **1993**, *14*, 1347.
(27) Shaik, S. S.; Schlegel, H. B.; Walfe, S. *Theoretical Aspects of Physical Organic Chemistry the SN2 Mechanism*; Wiley: New York, 1992; p 45.
(28) Harmony, M. D.; Nandi, R. N.; Tietz, J. V.; Choe, J.-I.; Getty, S. J.; Staley, S. W. *J. Am. Chem. Soc.* **1983**, *105*, 3947.
(29) Little, T. S.; Zhao, W.; Durig, J. R. *J. Raman Spectrosc.* **1988**, *19*, 479.
(30) Wong, M. W. *Chem. Phys. Lett.* **1996**, *256*, 391.
(31) Durig, J. R.; Tong, C. K.; Hawley, C. W.; Bragin, J. *J. Phys. Chem.* **1971**, 75, 1971.
(32) Demaison, J.; Burie, J.; Boucher, D.; Wlodarczak, G. *J. Mol. Spectrosc.* **1991**, *146*, 455.
(33) Kraka, E.; Cremer, D. *Chem. Phys. Lett.* **1993**, *216*, 333.
(34) Sastry, K. V. L. N.; Rao, V. M.; Dass, S. C. *Can. J. Phys.* **1968**, *46*, 959.
(35) Doubleday, C., Jr.; McIver, J. W.; Page, M. *J. Phys. Chem.* **1988**, *92*, 4367.
(36) Doering, W. von E.; Sachdev, K. *J. Am. Chem. Soc.* **1974**, *96*, 1168.
(37) Doughty, A.; Mackie, J. C. *J. Phys. Chem.* **1992**, *96*, 272.
(38) Saltiel, J.; Charlton, J. L. In *Rearrangements in ground and exited states*; de Mayo, P., Ed.; Academic Press: New York, 1980; Vol. 3, p 25.
(39) Eyring, H. *J. Chem. Phys.* **1935**, *3*, 107.
(40) Evans, M. G.; Polanyi, M. *Trans. Faraday Soc.* **1935**, *31*, 875.
(41) Kiefer, J. H.; Shah, J. N. *J. Phys. Chem.* **1987**, *91*, 3024.